THE JOURNAL OF PHYSICAL CHEMISTRY C
A JOURNAL OF THE AMERICAN CHEMICAL SOCIETY

pubs.acs.org/JPCC

Article

Fingerprinting the Hydration Products of Hydraulic Binders Using Snapshots from Time-Resolved *In Situ* Multinuclear MAS NMR Spectroscopy

Published as part of The Journal of Physical Chemistry virtual special issue "Advanced Characterization by Solid-State NMR and In Situ Technology".

Geo Paul, Enrico Boccaleri, Claudio Cassino, Daniela Gastaldi, Luigi Buzzi, Fulvio Canonico, and Leonardo Marchese*

Cite This: *J. Phys. Chem. C* 2021, 125, 9261–9272

Read Online

ACCESS | Metrics & More | Article Recommendations | Supporting Information

ABSTRACT: The very early hydration behavior of a hydraulic binder phase, ye'elimite, $Ca_4Al_6O_{12}SO_4$, in the absence and in the presence of calcium sulfate, has been investigated. A time-resolved *in situ* multinuclear magic angle spinning (MAS) nuclear magnetic resonance (NMR) spectroscopic suite involving ^1H and ^{27}Al MAS as well as two-dimensional ^{27}Al multiple quantum MAS (MQMAS) experiments has been employed to detect the transient species and to govern the sequence of hydration reactions and the subsequent formation of the hydration products. The results of the study show that the rates of formation of ye'elimite hydration products vary substantially according to the absence or the presence of calcium sulfate. Hydrated calcium sulfoaluminate phases such as ettringite and monosulfate as well as aluminum hydroxide gel have been detected during the various stages of hydration. The direct observation of various transient species during the hydration stages of calcium aluminates and calcium sulfoaluminates illustrates the potential of a newly designed time-resolved *in situ* ^1H MAS NMR experimental approach for fingerprinting phases and offers significant advantages over other established techniques in detecting transient species.

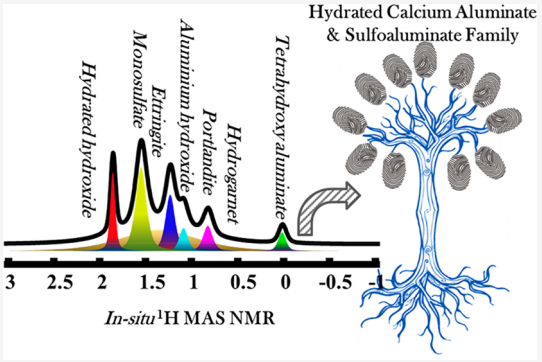

INTRODUCTION

Ye'elimite, also known as calcium sulfoaluminate, $Ca_4Al_6O_{12}SO_4$, is either the most important or key constituent in several high-functional hydraulic binders such as calcium sulfoaluminate (CSA), sulfobelitic, belite−ye'elimite−ferrite (BYF), and ternesite-based cements.[1,2] All these alternative binders have generated enormous interest lately due to their low carbon footprint and low energy demand compared to Portland cement (PC).[2,3] Important additional features of ye'elimite-based cements include fast setting and rapid hardening during early hydration as well as excellent chemical resistance and reduced shrinkage, making them desirable for the construction in offshore and coastal engineering.[4] Moreover, ye'elimite provides high early strength and shrinkage compensation when blended with Portland cement.[5] CSA clinker, first developed in the 1960s at the university of California at Berkeley by Alexander Klein,[6] is produced by burning a mixture of bauxite, limestone, and gypsum, in the right proportion, in a temperature range 1250−1350 °C which is at least 200 °C lower than that of Portland clinker production range, thus with a reduced energy demand and low greenhouse gas emissions.[7] The lower CaO content in ye'elimite is an additional environmental benefit as the reduced $CaCO_3$ demand in the CSA clinker production results in a lower CO_2 footprint. The CSA clinker manufacturing can actively be part of the circular economy by recycling the industrial byproducts and municipal wastes; thus, the resulting clinker is more grindable than the PC clinker, leading to further lower demand for energy.[8,9]

CSA-based binders may have variable compositions, but usually more than 50 wt % of ye'elimite is present in the clinker which is interground with around 20 wt % $CaSO_4$ (gypsum or anhydrite) resulting in cement.[10] Ye'elimite ($Ca_4Al_6O_{12}SO_4$) is a member of the sodalite family with the general formula $M_4[T_6O_{12}]X$, where M is a low charge caged cation (here

Received: February 2, 2021
Revised: April 8, 2021
Published: April 22, 2021

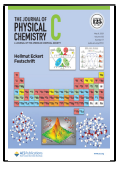

Ca^{2+}), T is the framework forming tetrahedral sites (here Al^{3+}), and X is a charge-balancing oxyanion (here SO_4^{2-}).[1] No single crystal structural solution has been reported in the literature for ye'elimite; however, recent powder diffraction studies based on X-ray, neutron, and synchrotron as well as the Rietveld refinement revealed the orthorhombic form (space group *Pcc*2) for stoichiometric ye'elimite at room temperature.[7,11,12] More recently, a detailed structural investigation by ^{27}Al MAS and MQMAS NMR spectroscopy conducted at different magnetic fields confirmed the orthorhombic *Pcc*2 structure of ye'elimite, illustrating the presence of eight crystallographically distinct Al sites (four with multiplicity 4 and four with multiplicity 2).[1]

It has long been known that the early hydration of CSA cement (also sulfobelitic, BYF, and ternesite-based cements) is greatly influenced by the behavior of its most reactive component, ye'elimite.[13] The general hydration reactions of ye'elimite have already been established. Hydration of ye'elimite in the absence of $CaSO_4$ results in the formation of monosulfate, an AFm (Al_2O_3−Fe_2O_3−monosulfate) family phase, along with amorphous aluminum hydroxide gel according to eq 1,

$$Ca_4Al_6O_{12}SO_4 + (12 + x + y)H_2O \rightarrow Ca_4Al_2(OH)_{12}SO_4\cdot xH_2O + 4Al(OH)_3\cdot yH_2O \quad (1)$$

When ye'elimite hydrates in the presence of gypsum, the Al_2O_3−Fe_2O_3−trisulfate (AFt) family phase, ettringite is formed according to eq 2 along with amorphous aluminum hydroxide gel,

$$Ca_4Al_6O_{12}SO_4 + 2CaSO_4\cdot 2H_2O + (34 + y)H_2O \rightarrow [Ca_6Al_2(OH)_{12}\cdot 26H_2O](SO_4)_3 + 4Al(OH)_3\cdot yH_2O \quad (2)$$

If insufficient gypsum is present, or if it is exhausted, ye'elimite will react with water to form monosulfate (eq 1).[14−16] Although the hydration of ye'elimite, either in the presence or in the absence of gypsum seems relatively simple, there are many parameters that can influence the early precipitation of hydrated aluminates. The formation of transient phases, both amorphous and crystalline, has been reported in earlier studies.[17−19]

Cement paste can be considered as a complex multicomponent, heterogeneous, and nonequilibrium solid-state material in which the early hydrated phases may undergo transient stability.[20] Understanding the molecular level chemistry that takes place at the anhydrous-solid/transient-liquid/hydrated-solid phases during the cement hydration is key to the development and improvement of many novel energy efficient, sustainable, and eco-friendly cements. In order to detect and to quantify the metastable phases formed in the first minutes of hydration at the solid/liquid/solid interface, a time-resolved *in situ* study is essential. Due to its unparalleled ability to equally detect and quantify amorphous, crystalline, disordered phases, and surface species as well as the unique advantage of probing the local structure at the molecular level, nonperturbing to the chemical state of the system, solid-state NMR spectroscopy is an ideal tool for *in situ* investigations.

Some of the earliest and most extensive studies on solid materials by *in situ* MAS NMR have been reported by Harris and co-workers.[21−24] In a recent study, Hughes et al., have reported the exploitation of *in situ* solid-state NMR spectroscopy to probe the early stages of hydration of calcium aluminate cement.[25] In a study by Chmelka and co-workers, the hydration of silicate materials has been measured by time-resolved solid-state NMR spectroscopy.[26] Similarly, Flatt and co-workers investigated the influence of aluminates on the hydration kinetics of tricalcium silicate by employing *in situ* MAS NMR spectroscopy.[27] Boccaleri and co-workers applied combined *in situ* MAS NMR spectroscopy and powder X-ray diffraction to investigate the binding mechanism for self-healing cementitious materials that can promote autonomous crack healing.[28]

Essentially, changes and formation of phases during hydration are often associated with changes in the environment of the surrounding nuclei. Therefore, any NMR-active nuclei can be monitored by *in situ* solid-state NMR spectroscopy, and the studies of different nuclei within the same material have the possibility to deliver a huge amount of complementary information. For the fast and routine *in situ* observations, both ^{1}H and ^{27}Al nuclei are favorable as they are naturally isotopically abundant and have a very high gyromagnetic ratio as well as very short relaxation times.

Anhydrous and hydrated aluminate phases can be easily distinguished in ^{27}Al NMR spectra as they resonate with distinguishable chemical shift ranges.[29] The resonances due to AlO_4 tetrahedra from anhydrous species will appear in the 50−100 ppm range while the hydrated aluminate phases possessing AlO_6 octahedra appear in the −10 to 15 ppm window. MAS alone is not sufficient to completely eliminate quadrupolar broadening, and the more complex two-dimensional techniques such as multiple-quantum magic angle spinning (MQMAS) NMR spectroscopy are required to obtain high-resolution spectra.[30,31] Another highly desirable NMR-active isotope for the study of solid-state materials is ^{1}H, due to its high natural abundance and the very high sensitivity.[32,33] High-resolution ^{1}H NMR spectra at moderate MAS frequencies can be obtained by isotopically diluting the protons with deuterium and could isolate the proton-bearing species from each other.[34] Thus, the highly resolved, robust, and quantitative *in situ* ^{1}H MAS NMR spectral data obtained can complement the *in situ* ^{27}Al MAS NMR data and help to determine the phase identity, composition, hydration rate, and transient species in hydrated hydraulic binders. In this study, we have employed the fast analysis capabilities of time-resolved *in situ* multinuclear MAS NMR spectroscopy to investigate the early hydration behavior of ye'elimite, both in the presence and in the absence of calcium sulfate. The ability to analyze wet samples by *in situ* MAS NMR spectroscopic investigations allowed us to monitor the phase assemblage evolution during the ye'elimite hydration, as a function of time.

METHODS

Sample Preparation and Characterization. Orthorhombic ye'elimite was prepared in the laboratory according to the procedure reported previously.[35] Ye'elimite was synthesized from stoichiometric amounts of $CaCO_3$ (Alfa Aesar, > 99%), Al_2O_3 (Merck, > 98%), and $CaSO_4\cdot 2H_2O$ (VWR International Ltd., > 99%) following the method reported by Winnefeld and Barlag.[35] After grinding, the mixture was sintered at 1350 °C for 4 h and brought back to room temperature rapidly. The obtained solid was studied by powder X-ray diffraction (Figure S1) that showed 96% pure orthorhombic ye'elimite phase. The remaining 4% was monocalcium aluminate.

https://doi.org/10.1021/acs.jpcc.1c00984
J. Phys. Chem. C 2021, 125, 9261−9272

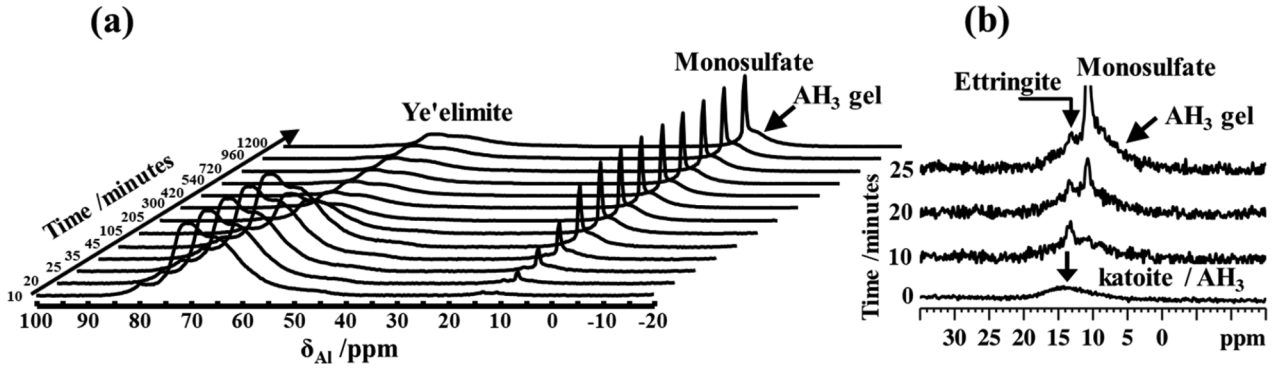

Figure 1. Stacked plot of time-resolved *in situ* ^{27}Al MAS NMR spectra (a) showing the rapid hydration of neat ye'elimite from the moment of deuterated water addition. The octahedral region of the ^{27}Al central transition MAS NMR spectra recorded under proton decoupling (b) highlighting the early formation ettringite, monosulfate, and AH_3 (aluminum hydroxide).

Before the *in situ* hydration procedure, orthorhombic ye'elimite and gypsum were thoroughly ground. The powdered neat ye'elimite or ye'elimite in combination with gypsum was packed into a Kel-F insert and hydrated with deuterated water (Sigma-Aldrich, 99.9%) using a water to solid ratio (w/s) of 0.5 and stirred for 1 min. After that, the Kel-F insert was rapidly sealed with plug and screw (to suppress the escape of fluids) and fitted into a 4 mm rotor and analyzed. The sample temperature (298 K) was set using a temperature control unit that was previously calibrated using lead nitrate. Data acquisition was started within 10 min of the initial contact of ye'elimite mix with deuterated water, selected patterns are plotted for clarity, and the time intervals between patterns were varied.

Time-Resolved *In Situ* Solid-State NMR Studies. Solid-state NMR spectra were acquired on a Bruker Avance III 500 spectrometer and a wide bore 11.75 T magnet with operational frequencies for ^{1}H and ^{27}Al of 500.13 and 130.32 MHz, respectively. A 4 mm triple resonance probe, in double resonance mode, with MAS was employed in all the *in situ* experiments and the samples were hydrated in a Kel-F insert that was fitted into a zirconia rotor and spun at a MAS rate of 13 kHz using a Bruker MAS III pneumatic unit. The ^{27}Al 1D MAS spectra have been acquired on large sweep width with small pulse angle ($\pi/12$) to ensure quantitative interpretation. In addition, central transition ^{27}Al MAS NMR spectra were acquired under high power proton decoupling conditions. The ^{27}Al 2D multiple quantum magic angle spinning (MQMAS) experiments have been acquired using zero-quantum filter (z-filter) 3QMAS pulse sequence.[30,31] The symmetric triple quantum excitation and conversion pulses of 52 and 208 kHz were used, respectively. The central transition selective soft pulse was 10 kHz with a z-filter delay of 20 μs. A 2D Fourier transformation followed by a shearing transformation (Bruker software, Topspin V3.6) gave pure adsorption mode 2D map; here the F1 axis projection gives isotropic spectra while the quantum-filtered MAS spectra was taken on the F2 axis and was reported according to the Bruker convention.

^{1}H MAS NMR spectra were collected with an excitation pulse of 100 kHz. In addition, a rotor-synchronized spin−echo sequence ($\pi/2-\tau-\pi-\tau-$acquisition) was also applied to record the ^{1}H NMR spectra with a delay time of 2008 ms. The delay time was chosen as an optimized compromise between the signal decay owing to relaxation and the resolution gain owing to longer delay times. When the longer echo times lead to the appearance of artifacts in the spectrum, this problem was overcome by using short echo times and cycling multiple times. The delays, d1, between accumulations were 1 and 2 s for ^{27}Al and ^{1}H, respectively. The chemical shifts are reported using δ scale and are externally referenced to the $Al(H_2O)_6^{3+}$ ion in 1.0 M $AlCl_3$ solution to 0.0 ppm for ^{27}Al and TMS to 0.0 ppm for ^{1}H. Each 1D ^{27}Al NMR spectrum was acquired in about 2 min (128 scans; recycle delay, 1 s) and ^{1}H NMR spectrum was acquired in 8 s (4 scans; recycle delay, 2 s). The 2D ^{27}Al MQMAS spectra were acquired only in selected time intervals, and the experiment times were varied according to the necessity of resolution enhancement in F1 dimension (typically, 128 *t1* increments with 48 scans and a recycle delay of 0.5 s, resulting in an experimental time of 51 min).

Additional ^{1}H NMR measurement was done in the liquid-state, and the spectrum was recorded using Bruker AVANCE NEO spectrometer equipped with an 11.74 T magnet (Larmor frequency of 500.38 MHz for ^{1}H) and a 5 mm double resonance Bruker Smartprobe and Bruker Smart Variable Temperature (BSVT) System for temperature control. During the wet impregnation, ye'elimite particles were soaked in excess deuterated water and stirred for a while. Later, the solid particles were allowed to settle down, followed by the extraction of the clear solvent and the submission to liquid-state NMR spectral recording. The ^{1}H NMR spectrum was recorded using a RF pulse of 3.1 kHz and 32 scans and a recycle delay of 3.5 s at 300 K after waiting 10 min for sample temperature stabilization. The chemical shifts are reported using the δ scale and are externally referenced to TMS at 0.0 ppm. ^{27}Al MAS NMR spectra are fitted for quantitative deconvolution of overlapping peaks.[36] The peaks associated with calcium aluminate and sulfoaluminate hydrates are described by quadrupolar line shapes. ^{27}Al MAS NMR spectra of ye'elimite, ettringite, monosulfate, and aluminum hydroxide have been published, and the quadrupolar coupling parameters and chemical shift values reported were used as an aid for the interpretation of NMR spectra and for the quantitative deconvolution study.[37−44]

RESULTS AND DISCUSSION

^{27}Al MAS and MQMAS NMR of Anhydrous Orthorhombic Ye'elimite. The ^{27}Al MAS NMR spectrum (Figure S2a) of anhydrous orthorhombic ye'elimite appeared as a broad and featureless center-band resonance as a consequence of the anisotropic quadrupolar interactions that arise from the eight different tetrahedral Al sites.[1,11,12] Although a very broad

https://doi.org/10.1021/acs.jpcc.1c00984
J. Phys. Chem. C 2021, 125, 9261−9272

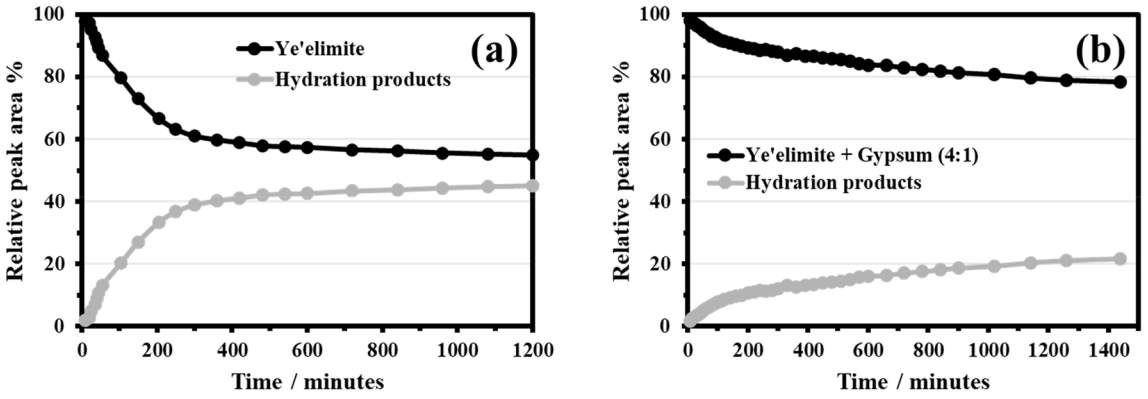

Figure 2. Time dependence of the peak areas due to reactant (ye'elimite) and hydration products (sum of ettringite, monosulfate, and aluminum hydroxide gel) derived from the time-resolved *in situ* ^{27}Al MAS NMR spectra showing the variable hydration rate of neat ye'elimite (a) and ye'elimite/gypsum mix (4:1) (b). The areas of integration are from 100 to 30 ppm and from 30 to −10 ppm for reactant and products, respectively.

and weak resonance has been detected in the octahedral region, it is not considered as part of the ye'elimite structure and is instead attributed to traces of surface hydration. We have also employed ^{27}Al MQMAS NMR techniques to elucidate the structural details of anhydrous ye'elimite (Figure S2b). A local ^{27}Al site disorder in ye'elimite is noted from the NMR study, and further details are given in the Supporting Information.

Hydration of Orthorhombic Ye'elimite in the Absence of Calcium Sulfate. The time-resolved *in situ* ^{27}Al MAS NMR spectra recorded on the ye'elimite pastes hydrated for up to 20 h are shown in Figure 1a. The first spectrum has been recorded within 10 min of deuterated water contact and the first three ^{27}Al central transition MAS NMR spectra (octahedral region) recorded under proton decoupling are shown in Figure 1b. For comparison purpose the ^{27}Al MAS NMR spectrum of anhydrous ye'elimite is shown (time = 0). A very broad asymmetric peak with chemical shift in the range 5−17 ppm is detected in the anhydrous ye'elimite and is attributed to transient hydrated aluminate phases formed as a result of minor surface hydration. Although the studied ye'elimite sample has a purity of 96%, traces of monocalcium aluminate ($CaAl_2O_4$) are present as well. Therefore, the origin of surface hydration could be either due to ye'elimite or due to monocalcium aluminate. Hydration of monocalcium aluminate above 296 K results in the cubic calcium aluminum hydroxide phase katoite, $Ca_3Al_2(OH)_{12}$, with garnet structure (also known as hydrogarnet) and aluminum hydroxide. On the other hand, monosulfate and aluminum hydroxide are the ye'elimite hydration products.

The formation of phases such as hydrogarnet, monosulfate, and aluminum hydroxide are expected, and ^{27}Al MAS NMR spectroscopy is an excellent tool to detect both amorphous and crystalline aluminate phases, concurrently. Crystalline hydrogarnet would appear as a relatively broad peak centered at around 12.4 ppm while aluminum hydroxide in the form of gibbsite would give two broad resonances in the range 8−14 ppm.[38] Moreover, ^{27}Al in amorphous phases can appear as a broad and featureless band in the spectrum as a result of the anisotropic and quadrupolar interactions that affect the nuclear spins. Therefore, the very broad asymmetric peak in the range 5−17 ppm in Figure 1b (time = 0) is attributed to contributions from amorphous aluminum hydroxide and hydrogarnet originated from the hydration of monocalcium aluminate. This assignment will be further corroborated with the ^{1}H MAS NMR data.

Upon initial hydration (time = 10 min), changes are seen in the octahedral region of the spectrum, Figure 1b, with the growth of two new resonances is being evident, a narrow peak at around 13.2 ppm and a broader peak further upfield (lower ppm values). It is not straightforward to distinguish the broader peak from that at the 5−17 ppm detected in the anhydrous sample, but we can confidently say that the upfield shift indicates the disappearance of a phase. We believe that the hydrogarnet component has been transformed into a new phase and appeared as a narrow peak detected at 13.2 ppm and is assigned to ettringite, $\{Ca_6[Al_2(OH)_{12}]24H_2O\}(SO_4)_3\cdot 2H_2O$. The broader one is associated with amorphous aluminum hydroxide gel, $Al(OH)_3\cdot xH_2O$. As the hydration of ye'elimite is initiated, sulfate ions become available and can react with the hydrogarnet, forming early ettringite. The formation of ettringite is not expected during the hydration of neat ye'elimite in the absence of $CaSO_4$ (eq 1).[45−47] However, there are some reports in the literature that proposed a different reaction pathway for early ye'elimite hydration.[17,18] As can be seen from eq 3, early ye'elimite hydration can lead to the precipitation of ettringite and calcium aluminate decahydrate along with aluminum hydroxide.

$$3Ca_4Al_6O_{12}SO_4 + [(6 \times 1.84) + 74 + y]H_2O \rightarrow [Ca_6Al_2(OH)_{12}\cdot 26H_2O](SO_4)_3 + 6[CaAl_2(OH)_8(H_2O)_2\cdot 1.84H_2O] + 4Al(OH)_3\cdot yH_2O \quad (3)$$

It has been suggested that calcium aluminate decahydrate along with aluminum hydroxide could precipitate in amorphous forms.[17,18] If this reaction pathway occurs in our sample, substantial decrease in the ye'elimite content along with a significant increase in calcium aluminate decahydrate would be expected. However, no such changes are witnessed in the ^{27}Al MAS NMR spectra at early stages of hydration. Moreover, the experiment has been carried out at 298 K where the formation of calcium aluminate decahydrate is restricted, as stated earlier. Monocalcium aluminate decahydrate has a unique $^{27}AlO_6$ site with an isotropic chemical shift (δ_{iso}) at 10.2 ppm and quadrupolar coupling constant (C_Q) of 2.4 ± 0.2 MHz.[38] Therefore, according to our ^{27}Al MAS NMR data, we cannot confirm the formation of monocalcium aluminate

https://doi.org/10.1021/acs.jpcc.1c00984
J. Phys. Chem. C 2021, 125, 9261−9272

decahydrate at very early ages, and we exclude the occurrence of the reaction pathway according to eq 3. Similar observations have been recently reported.[48]

The crystal structure of aluminum hydroxide (in the form of gibbsite) contains two nonequivalent ^{27}Al sites in octahedral environments and in the ^{27}Al MAS NMR, the two resonances associated with them overlap and display a featureless spectrum.[38] However, the aluminum hydroxide gel detected in our study displayed a very broad asymmetric line shape, without resolving the two resonances associated with the two nonequivalent ^{27}Al sites, illustrating the high structural disorder in the phase.[37,49] Being one of the main hydration product of ye'elimite based cements, aluminum hydroxide gel attracts enormous interest among researchers, and we assert that they may contribute to the strength evolution.[50] As the hydration progressed further (time = 20 min), a new narrow peak appears with δ_{cg} at around 10.7 ppm and is attributed to the formation of monosulfate, $[Ca_4Al_2(OH)_{12}](SO_4)\cdot xH_2O$, with x = 5, 6, and 7.5.[5,43] In addition, the broader peak assigned to amorphous aluminum hydroxide gel increased its intensity as the hydration progressed. However, we note that the contribution due to ettringite (13.2 ppm) remains unchanged. The resonances due to monosulfate and amorphous aluminum hydroxide gel grew over time relatively quickly, consistent with the fast hydration of ye'elimite.

Over the next 1200 min, the *in situ* ^{27}Al MAS NMR data revealed no changes in the phases present, although the relative intensities of the resonance peaks and therefore the quantity of these phases did vary (Figure 1a). From the *in situ* NMR data, the rate of ye'elimite hydration as well as the kinetics of product formation can be monitored as a function of time (Figure 2, parts a and b). Integrating the area under the NMR peaks due to reactant (ye'elimite) as well as products (monosulfate and aluminum hydroxide gel) and plotting against time yield kinetic information.

Figure 2a presents the time dependence of peak areas due to ye'elimite, hydrated in the absence of gypsum, as well as monosulfate and aluminum hydroxide gel, illustrating the kinetics under different time periods. The very rapid hydration rate of ye'elimite upon initial contact with deuterated water is clearly evident from the sharp growth of products, and it continues up to 300 min. However, beyond that, the growth is retarded. Consequently, more than 50% of anhydrous ye'elimite remained in the paste, and the slow hydration rate is probably due to the low water to ye'elimite ratio employed in the experiment. It is well-known that the lower amount of water retards the ye'elimite hydration rate, and the water content in our study has been less than the required stoichiometric amount for a complete hydration according to eq 1.[14] As majority of the water is consumed for the early formation of monosulfate and aluminum hydroxide gel (water bearing phases); lack of sufficient water delayed the ye'elimite hydration further. This topic will be augmented while discussing the ^{1}H MAS NMR data.

Figure 3, top panel, shows the octahedral region of the ^{27}Al central transition MAS NMR spectrum recorded under proton decoupling of ye'elimite hydrated for 1200 min along with the deconvoluted spectrum with individual contributions from each ^{27}Al site. While the resonance peak due to monosulfate exhibited typical quadrupolar line shape, a broad featureless asymmetric peak, without exhibiting any specific quadrupolar line shape, is displayed by amorphous aluminum hydroxide gel. The combined simulated line shape, resulting from the two

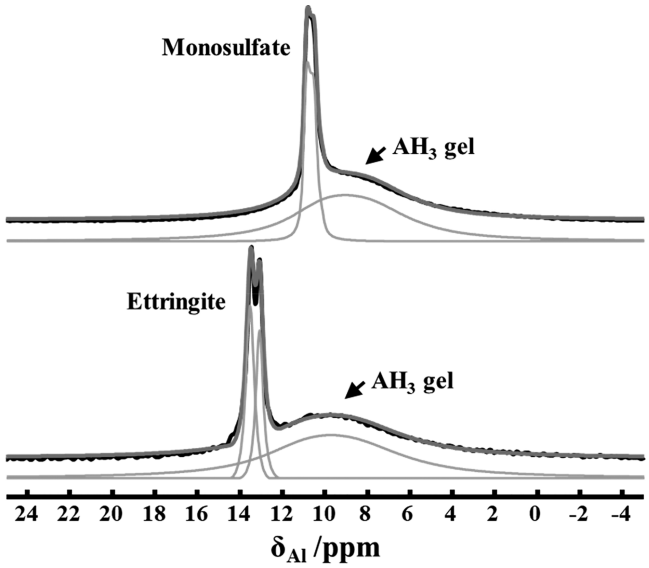

Figure 3. ^{27}Al MAS NMR spectra (octahedral region), recorded under proton decoupling, of the hydrated ye'elimite samples (black) along with the deconvoluted spectrum (dark gray) and the individual contribution from each ^{27}Al sites (light gray). The samples have been hydrated for 20−24 h: neat ye'elimite (top) and ye'elimite/gypsum mix (4:1) (bottom). AH_3, aluminum hydroxide. The corresponding quadrupolar coupling parameters and chemical shifts are given in Table 1.

phases, is in excellent agreement with the experimental spectrum. The estimated ^{27}Al isotropic chemical shift and quadrupolar coupling parameters are shown in Table 1. We note that the values are slightly different from those reported in the literature and are either due to the differences in the water content in these phases or due to the presence of deuterated hydroxyls and water.[38] Different monosulfate phases, $[Ca_4Al_2(OH)_{12}](SO_4)\cdot xH_2O$, have been identified in the ye'elimite hydration products, with x = 5, 6, and 7.5, and in general, AFm phases have a very rich intercalation chemistry and structural diversity.[51,52] Moreover, for a disordered multicomponent material, each spectrum contains unresolved intensity from ^{27}Al sites with ranges in quadrupolar coupling parameters and chemical shifts; therefore, the results from the fits are not unique. However, the approach yields some estimates.

We show in Figure 4a the ^{27}Al MAS and in 4b the 2D ^{27}Al MQMAS NMR spectra of hydrated ye'elimite along with the projections onto the isotropic (F1) and quantum filtered MAS (F2) dimensions. The spectrum has been recorded on a ye'elimite paste hydrated for 1200 min. It is clear that the spectrum contains two peaks, one sharp 2D resonance with characteristic quadrupolar line shape due to monosulfate (marked by an arrow) as well as a very broad and unresolved component spread over both dimensions, without any specific quadrupolar line shape, attributed to amorphous aluminum hydroxide gel. The 2D map displays the well-defined differences in these phases due to their diverse quadrupolar parameters and chemical shift distributions. The 2D peak associated with monosulfate appeared closer to the chemical shift axis (diagonal dotted line) with very narrow line width along both F1 and F2 axis implying smaller quadrupolar couplings and very limited chemical shift distributions. On the contrary, the 2D peak due to amorphous aluminum hydroxide gel spreads in both dimensions mainly due to second order

https://doi.org/10.1021/acs.jpcc.1c00984
J. Phys. Chem. C 2021, 125, 9261−9272

Table 1. Experimental ^{27}Al Quadrupolar Coupling Constant (C_Q), Asymmetry Parameter of the Electric Field Gradients (η_Q), Isotropic Chemical Shifts (δ_{iso}), and Center-of-Gravity Peak (δ_{cg}) Position of the Various Phases Detected in the Ye'elimite Samples Hydrated for 20−24 h

	phase	C_Q (MHz)	η_Q	δ_{iso} (ppm)[a]	δ_{cg} (ppm)[b]
ye'elimite	monosulfate	1.06 ± 0.2	0.25 ± 0.05	11.1 ± 0.1	10.7 ± 0.1
	AH_3 gel	2.70 ± 0.2	0.10 ± 0.05	11.4 ± 0.1	8.9 ± 0.1
ye'elimite/gypsum	AH_3 gel	2.77 ± 0.2	0.10 ± 0.05	12.3 ± 0.1	9.7 ± 0.1
	ettringite 1	0.37 ± 0.2	0.25 ± 0.05	13.6 ± 0.1	13.5 ± 0.1
	ettringite 2	0.38 ± 0.2	0.24 ± 0.05	13.1 ± 0.1	13.1 ± 0.1

[a]Referenced to $Al(H_2O)_6^{3+}$ ion in 1.0 M $AlCl_3$ solution at 0.0 ppm, [b]At 11.75 T.

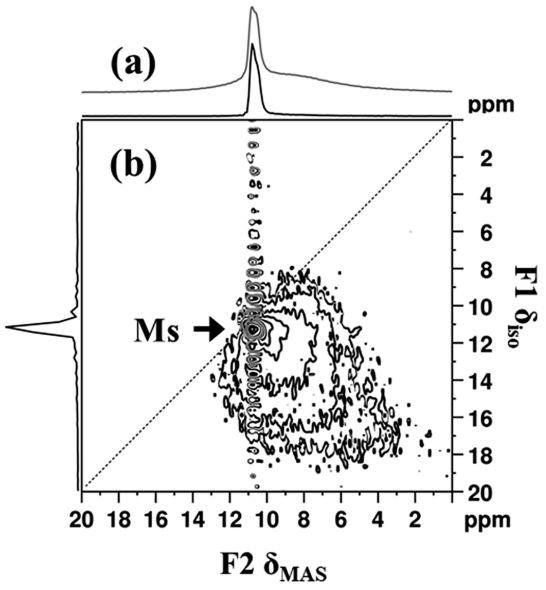

Figure 4. ^{27}Al central transition MAS NMR spectrum (a) and the contour plot of 2D t_1 rotor-synchronized ^{27}Al zero-quantum filter MQMAS NMR spectrum (b) of the hydrated ye'elimite (time = 1200 min). The projections onto the isotropic (F1) and quantum filtered MAS (F2) dimensions correspond to summations over the 2D spectra. The dotted line in the 2D spectrum indicates the chemical shift axis. An arrow highlights the 2D peak due to Ms (monosulfate).

quadrupolar broadening (parallel to the F2 axis) and the distribution of chemical shifts (parallel to the F1 axis) accentuating the very high disorder in this phase. Bertola and co-workers have demonstrated that 2D ^{27}Al MQMAS NMR experiments can distinguish amorphous aluminum hydroxide gel from amorphous third aluminate hydrate.[53]

From the MQMAS NMR data, it can be summarized that during the hydration of ye'elimite, a highly ordered monosulfate and extremely disordered amorphous aluminum hydroxide gel are formed.

Hydration of Orthorhombic Ye'elimite in the Presence of Gypsum. The time-resolved *in situ* ^{27}Al MAS NMR spectra recorded from ye'elimite paste in the presence of gypsum (with a ye'elimite/gypsum ratio 4:1), hydrated for up to 24 h are shown in Figure 5a. The first spectrum has been recorded within 9 min of deuterated water contact, and the ^{27}Al central transition MAS NMR spectra (octahedral region) recorded under proton decoupling along with the spectrum of anhydrous ye'elimite (time = 0) are shown in Figure 5b. The *in situ* NMR data revealed a similar phase development to the previous sample at very early hydration stages (up to 19 min). Ettringite and amorphous aluminum hydroxide gel are the main hydration products, as expected, when ye'elimite reacts with water in the presence of calcium sulfate according to eq 2. Monocalcium aluminate decahydrate has never been detected in this system. The resonance intensity due to both ettringite and amorphous aluminum hydroxide gel grew over time, however, rather very slowly. A comparison between Figures 5a and 1a demonstrate the extent of retardation in the early ye'elimite hydration in the presence of gypsum. The rate of hydration products formation shown in Figure 2b demonstrates that it took more than 1000 min for 20% of the ye'elimite to react in the presence of gypsum. The hydration of ye'elimite continued up to the end of the experimental study.

Interestingly, the resonance due to ettringite starts to appear as a "doublet" in the ^{1}H decoupled ^{27}Al MAS NMR spectra revealing the presence of two distinct AlO_6 octahedral sites. The "doublet peak" line shape remained in all the spectra recorded throughout the study period (24 h). A spectral fitting (Figure 3, bottom panel) revealed the two resonances at δ_{iso} =

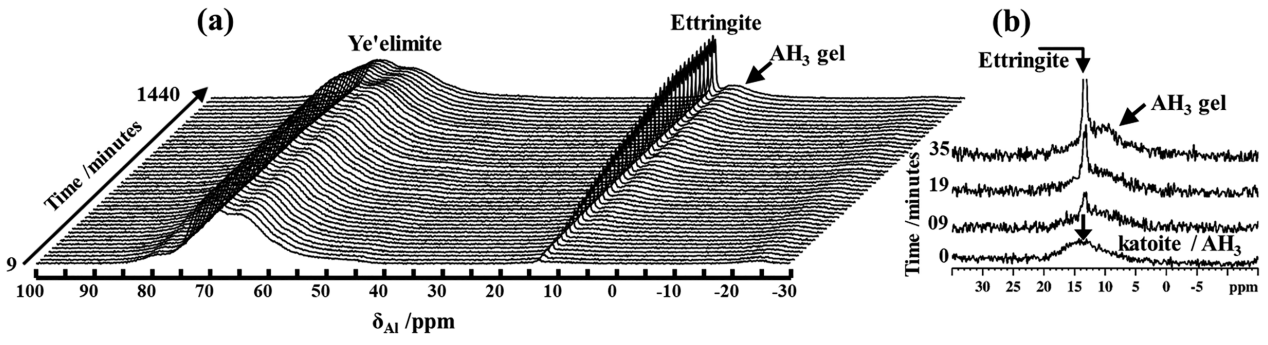

Figure 5. Stacked plot of time-resolved *in situ* ^{27}Al MAS NMR spectra (a) showing the retarded hydration of ye'elimite/gypsum mix (4:1). The octahedral region of the ^{27}Al central transition MAS NMR spectra recorded under proton decoupling (b) highlighting the early formation of ettringite and AH_3, aluminum hydroxide.

https://doi.org/10.1021/acs.jpcc.1c00984
J. Phys. Chem. C 2021, 125, 9261−9272

13.6 ± 0.1 and 13.1 ± 0.1 ppm and each exhibited a line width of approximately 64 ± 3 Hz with a relative intensity ratio of 1:1. A recent study has reported similar observations of two distinct Al sites for ettringite, by employing 1D and 2D ^{27}Al MAS NMR at an ultrahigh magnetic field (22.3 T), thereby supporting the trigonal model (space group $P31c$) for the crystal structure of ettringite.[39] The combined simulated line shape, resulting from the three sites (two of them belong to ettringite), is in excellent agreement with the experimental spectrum. We note that the ^{27}Al isotropic chemical shift and quadrupolar coupling parameters for amorphous aluminum hydroxide gel are slightly different between the two samples (Table 1) and is probably due to the differences in the microstructural environment or due to the variable water and calcium content in this phase.[54−56] Moreover, the values for the two distinct AlO_6 octahedral sites in ettringite are in excellent agreement with those reported by Skibsted and co-workers.[39]

Time-Resolved *In Situ* ^{1}H MAS NMR Study of the Hydration of Ye'elimite. Protonic species are mainly found in three different states in a cement paste. When water is added to anhydrous cement, it can remain as physical water or form hydroxyl groups or take the form of structural hydrate water. In addition, protons can be found in the form of hydroxide ions, micro-/nanopore water, interlayer water, and surface adsorbed water. Generally, the hydroxyl groups belonging to the hydrated cement phases with different origins and chemical environments appear in the large ^{1}H chemical shift scale. Depending on the presence or absence of hydrogen-bonding environments, they experience highly flexible chemical shifts. The unambiguous peak assignments in this study are based on control experiments and previously reported data. ^{1}H MAS NMR data can not only reveal the different protonic species present in the cement pastes but also be used to quantitatively determine the kinetics of hydration process. We have employed time-resolved *in situ* ^{1}H MAS NMR for the determination of the speciation of the protons within the ye'elimite hydration products. The fingerprint region of the ^{1}H MAS NMR spectrum, falling in the −1 to 3 ppm chemical shift range, can be exploited to map common hydrated calcium aluminate phases through their hydroxyl groups.

Figure 6a shows the ^{1}H spin−echo MAS NMR spectrum of neat ye'elimite obtained with a MAS rate of 15 kHz. Inspection of the spectrum reveals that different protonic species are already present in neat ye'elimite before the contact with bulk water. Mainly, three sharp peaks at around 1.25, 0.85, and at −0.05 ppm as well as one relatively broad peak in the range −1.0 to −0.4 ppm are resolved in the spectra. The other broad peak in the range 8 to −4 ppm is mainly due to the MAS probe background, although the contributions from hydrogen-bonded protons such as in aluminum hydroxide gel cannot be excluded. The most intense peaks at 1.25 and 0.85 ppm are tentatively attributed to the hydroxyls of calcium hydroxide.[26,57] To further support this assignment, we have recorded a ^{1}H NMR spectrum on hydrated calcium oxide. Indeed, the proton spectrum shown in Figure 6b displays multiple resonances in the range 0.6 and 1.4 ppm for hydrated calcium oxide, confirming the above assignment. According to the previous reports, different Ca−OH type hydroxyls may exist, depending on the pH conditions.[57,58] The most prevalent species in alkaline conditions are >Ca−OH and >$Ca(OH)_2^-$. Portlandite, the crystalline form of calcium hydroxide, may also appear in the same chemical shift range.

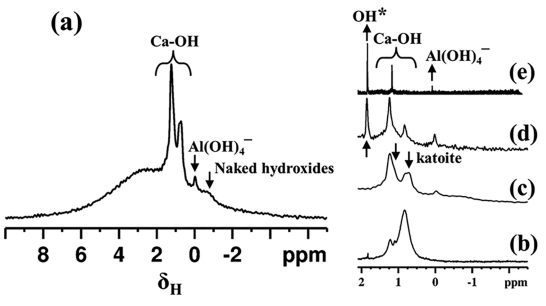

Figure 6. ^{1}H spin−echo MAS NMR spectrum (a) of anhydrous orthorhombic ye'elimite recorded with a MAS rate of 15 kHz. ^{1}H spin−echo MAS NMR spectrum of hydrated CaO (b), the fingerprint region of the spectra for anhydrous orthorhombic ye'elimite before hydration (c), and after being hydrated for 10 min (d). The liquid-state ^{1}H NMR spectrum of ye'elimite (e). $[Al(OH)_4]^-$, tetrahydroxy aluminate anion; OH* represents hydrated hydroxide ions.

In the ^{1}H NMR spectrum (Figure 6, parts a and c), there is the presence of a sharp peak at around −0.05 ppm with relatively lower intensity and is attributed to $[Al(OH)_4]^-$ species. At basic pH conditions, tetrahydroxy aluminate anions are prevalent and during the hydration of ye'elimite its concentration can increase with time. However, the presence of tetrahydroxy aluminate anions in anhydrous ye'elimite demonstrate, irrefutably, the initiation of surface hydration process. This hypothesis is further confirmed by recording the spectra of hydrated ye'elimite in both solid and liquid state (Figure 6, parts d and e). The most striking feature of Figure 6a is the observation of a low intensity broad peak in the range −1.0 to −0.4 ppm and has been assigned to the presence of residual naked hydroxide ions. The origin and form of the existence of the naked OH^- ions in anhydrous ye'elimite is not completely clear. One possible explanation is the presence of oxide ions (O^{2-}) in the cavities of sodalite framework of neat ye'elimite sample due to sulfur volatilization. The O^{2-} ions, that are possibly substituting some of the sulfate anions in a ye'elimite sample, are highly reactive and when exposed to atmospheric water vapor act as a basic oxide and readily yield hydroxide ions according to eq 4. Hydroxide species are very well-known as guest ions in aluminosilicate sodalites (e.g., hydroxysodalite).[59−61] Since the O^{2-} ions are randomly occluded in the cavities of ye'elimite structure, the resulting hydroxide ions are heterogeneously distributed locally reflecting as a broad resonance peak in the ^{1}H NMR spectrum.[26] Moreover, their highly reactive nature could initiate surface hydration and impact the local molecular environments. In addition, the short-range disorder in the ye'elimite structure is likely to be related to site occupancies where sulfate ions are displaced as has been pointed out during the discussion of ^{27}Al MQMAS NMR data.

$$O^{2-} + H_2O \rightarrow 2OH^- \quad (4)$$

In Figure 7a, we present the stacked plot of the time-resolved *in situ* ^{1}H MAS NMR spectra showing exemplar results for the early hydration behavior of neat ye'elimite together with fingerprint chemical shifts for hydration products and transient species (Figure 7b). A thermogravimetric analysis of neat ye'elimite sample (Figure S3) revealed that less than 0.2% of water is present in the form of surface hydration. It is expected that protons from the surface hydrated species would give signals sooner than the protons supplied by the D_2O

https://doi.org/10.1021/acs.jpcc.1c00984
J. Phys. Chem. C 2021, 125, 9261−9272

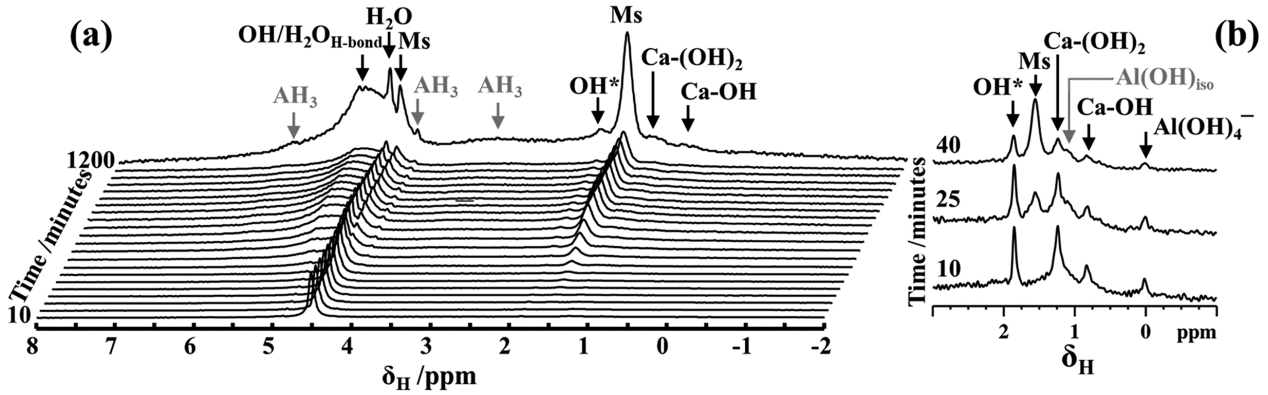

Figure 7. Stacked plot (a) of time-resolved *in situ* ^{1}H MAS NMR spectra showing the rapid hydration of neat ye'elimite from the moment of deuterated water addition. The fingerprint region of the *in situ* ^{1}H spin−echo NMR spectra (b) highlighting the early formation of monosulfate (Ms). $[Al(OH)_4]^-$, tetrahydroxy aluminate anion; $Al(OH)_{iso}$, isolated AlOH; AH_3, aluminum hydroxide gel; OH* represents hydrated hydroxide ions.

impurities. Upon initial contact with bulk deuterated water (time = 10 min), the main resonance in the ^{1}H MAS NMR spectrum has been an intense peak at 4.5 ppm and is due to bulk water. However, minor changes have been begun to display in the fingerprint region of the spectrum as shown in the *in situ* ^{1}H spin−echo NMR spectra (Figure 7b). The first spectrum has been recorded at around 10 min after contact with deuterated water and showed four sharp resonances at 1.85, 1.25, 0.85, and 0.0 ppm. Contributions due to hydroxyls from calcium hydroxide are at around 1.25 and 0.85 ppm while tetrahydroxyaluminate anion would appear at around 0.0 ppm; therefore, their attributions are straightforward. However, the detection of a sharp peak at 1.85 ppm in the spectrum is surprising.

The ^{27}Al MAS NMR data (Figure 1b) clearly confirmed the transformation of amorphous hydrated aluminates detected in anhydrous ye'elimite to ettringite and aluminum hydroxide upon contact with deuterated water. Therefore, one would expect that the peak at 1.85 ppm in the proton NMR spectrum could be due to ettringite and/or aluminum hydroxide. However, resonance peaks due to hydroxyls or water present in the above two phases would appear at different chemical shift values and their contributions to this peak has been excluded. A closer examination of the ^{1}H NMR spectra (Figure 6, parts c and d) of anhydrous and hydrated ye'elimite revealed the appearance of striking differences upon contact with deuterated water. In addition to the ^{1}H peaks associated with hydrated calcium hydroxide, two more peaks at 0.65 and 1.1 ppm are present in the anhydrous sample (marked by down-arrows). The peak at 0.65 ppm disappears upon contact with deuterated water, and a new narrow ^{1}H peak appears at 1.85 ppm (marked by an up-arrow). Therefore, the proton contributions at 0.65 ppm in the spectrum of anhydrous ye'elimite are attributed to hydrogarnet/katoite $[Ca_3Al_2(OH)_{12}]$ and the one at 1.1 ppm assigned to terminal AlOH groups of aluminum hydroxide $[Al(OH)_3]$.[62,63] A sharp proton resonance peak is an indication of highly mobile species, therefore, can be extracted into the solution state. We, therefore, recorded a ^{1}H NMR spectrum of anhydrous ye'elimite (using wet impregnation) in the liquid-state and is shown in Figure 6e. Indeed, the detection of an intense peak at 1.85 ppm in the liquid-state ^{1}H NMR spectrum confirms their mobile nature.

The origin and the nature of these mobile protonic species has been further investigated and the most likely source would be hydrogarnet (katoite). It has a cubic structure where each SiO_4 group of grossular $Ca_3Al_2(SiO_4)_3$ is replaced by an $(OH)_4$ group, arriving at hydrogrossular (katoite) $Ca_3Al_2[(OH)_4]_3$ compound. The hydroxyls of katoite would give a ^{1}H NMR peak at around 0.65 ppm. However, in the presence of abundant amount of anions such as sulfates in solution, katoite is unstable, resulting in its dissolution and readily transforming to ettringite.[64] Such a process could be accompanied by the presence of ion pairs involving Ca^{2+} and hydroxide ions as well as water leading to hydrated species. Therefore, the peak at 1.85 ppm in the ^{1}H NMR spectrum is attributed to hydrated hydroxyl species (marked as OH* in Figures 6 and 7).

In the ^{1}H NMR spectra (Figure 7b), an unresolved broad peak in the range 0.5−2 ppm is also visible and is attributed to ettringite. This assignment would be further clarified while discussing the hydration of ye'elimite/gypsum mix sample. At about 25 min, a sharp peak at around 1.55 ppm started to appear, and its intensity kept on growing and is assigned to monosulfate, in agreement with the *in situ* ^{27}Al MAS NMR data. In parallel, at 4.43 ppm, a shoulder upfield to the resonance peak due to bulk water also emerges and is also attributed to monosulfate. The former is associated with the hydroxyl protons while the latter is due to coordinated and/or hydrogen-bonded water present in monosulfate. An additional resonance at 1.1 ppm, in the fingerprint region, appears in parallel with the emergence of monosulfate and is attributed to isolated AlOH, in concordance with eq 1. Interestingly, another striking feature has also been observed to appear as a peak at around 8.4 ppm and is due to clustered Al_2OH sites.[65] These isolated AlOH and clustered Al_2OH sites are the molecular precursors for the formation of aluminum hydroxide gel, $Al(OH)_3{\cdot}xH_2O$.

As the hydration progressed, no relative increase in the intensity of resonance peaks due to OH*, ettringite, calcium hydroxide, and $[Al(OH)_4]^-$ ions are noted, however, a decrease in the amount of bulk water is evidenced. Additional peaks started to emerge in the downfield range and are attributed to aluminum hydroxide gel. Its amorphous nature can be easily distinguished from the crystalline gibbsite as the characteristic ^{1}H NMR peaks associated with the latter have been absent in the spectra. Gibbsite has a sheetlike structure built from $Al_2(OH)_6$ octahedra connected through the edges,

https://doi.org/10.1021/acs.jpcc.1c00984
J. Phys. Chem. C 2021, 125, 9261−9272

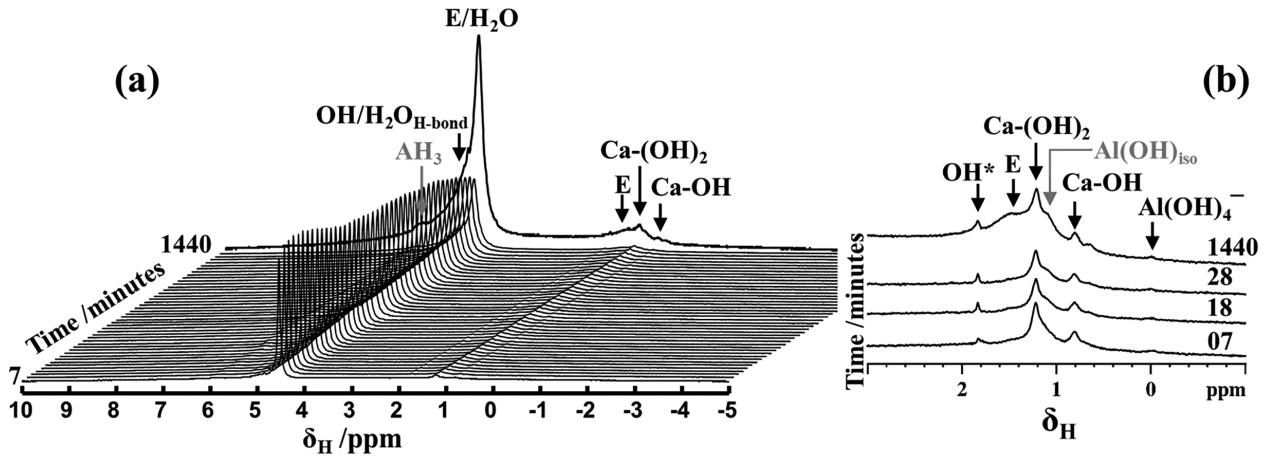

Figure 8. Stacked plot (a) of time-resolved *in situ* ^{1}H MAS NMR spectra showing the hydration of ye'elimite/gypsum mix (4:1) from the moment of deuterated water addition. The fingerprint region of the *in situ* ^{1}H spin−echo NMR spectra (b) highlighting the formation of ettringite (E). $[Al(OH)_4]^-$, tetrahydroxy aluminate anion; $Al(OH)_{iso}$, isolated aluminols; AH_3, aluminum hydroxide gel; OH* represents hydrated hydroxide ions.

where the center is occupied by the Al^{3+} cations and coordinated to hydroxyl groups located in the vertices. Both sides of the 2D layers are hydroxylated and can be distinguished as inter- and intralayer hydroxyls which take part in hydrogen-bonding networks that result in a stacked sheetlike structure. Since all the six hydroxyls in gibbsite participate in either intra- (4.2, 5.7, and 5.9 ppm) or interlayer (2.4, 3.8, and 6.9 ppm) hydrogen bonding, their proton chemical shifts are downfield shifted from the fingerprint region.[66]

In the present study, signatures of intralayer hydroxyls of aluminum hydroxide gel are detected in the *in situ* ^{1}H NMR spectra at 4.2 and 5.8 ppm as relatively sharp resonances while a broad peak in the range 2 to 4 ppm is probably due to interlayer hydroxyls (Figure 7a). In addition, two very broad resonances in the ranges 3.8 to 5.8 ppm and 5 to 8 ppm have been observed as the hydration further progressed. These broad resonances are assigned to protons from hydroxyls and water molecules that are involved in hydrogen-bonding networks. The emergence of these broad proton resonances in parallel with the reduction in the intensity of resonance due to bulk water confirm the formation of a gel-like structure involving aluminum hydroxide and water. However, the chemical shifts of protons involved in hydrogen-bonding networks present in other hydrated phases fall in the same range; therefore, their contributions cannot be excluded.

In the ye'elimite/gypsum mix, two main processes control the hydration phenomena, the dissolution of gypsum as well as ye'elimite and the precipitation of aluminate hydrates. The *in situ* ^{1}H NMR data shown in Figure 8a deliver direct evidence for both the processes. It can be seen that no distinct change occurs in the fingerprint region of the spectra for the first 28 min as the main resonance peaks are related to calcium hydroxide and OH* (Figure 8b). However, a substantial difference in their intensity ratios is clearly noticeable when compared with a neat ye'elimite hydrated sample (Figure 7b). This marked increase in the intensity of calcium hydroxide peaks in ye'elimite/gypsum mix is a direct proof that gypsum is preferentially hydrated over ye'elimite at very early hydration stages. Although an increase in the intensity of a peak, as a shoulder at 1.1 ppm, is clearly evident at early hydration stages, they are due to isolated aluminols.

On the other hand, the most intense peak in the ^{1}H MAS NMR spectra is attributed to water which appear at 4.55 ppm (Figure 8a). More importantly, the intensity of this peak grows over time for the first 28 min, contrary to what would be expected as water could be consumed during the hydration process of ye'elimite and decreases in quantity over time. This peculiar behavior can be explained as the dissolution of $CaSO_4 \cdot 2H_2O$, which would release the water of crystallization and add more protons to an otherwise deuterated water-based reservoir system. After 28 min of hydration, a gradual decrease in the intensity as well as broadening of this peak is visible and is continued until the end of the experiment time. Water molecules associated with various hydrated aluminate phases contribute to this peak, in addition to the broad peak in the range 4−8 ppm, responsible for hydrogen-bonded species.

Unlike in the ^{1}H MAS NMR spectra of neat ye'elimite hydration where the contribution due to hydroxyls of monosulfate started to appear very early in the fingerprint region at 1.55 ppm as a sharp peak (Figure 7b), no such band has been visible for gypsum-based systems. On the other hand, it is evident from the ^{27}Al MAS NMR data (Figure 5) that ettringite started to appear from the very early hydration stages. The 12 hydroxyls present per unit formula of ettringite, $\{Ca_6[Al_2(OH)_{12}]24H_2O\}(SO_4)_3 \cdot 2H_2O$, should appear in the fingerprint region of the ^{1}H NMR spectra. The apparent invisibility of ettringite hydroxyls at very early hydration stages can be either due to their rapid chemical exchange with water or their existence in a hydrogen-bonded state; both cases leading to a downfield shift of proton resonances. However, factors such as low intensity and inhomogeneous line broadening or the existence in a mostly deuterated state could also be responsible for their absence the ^{1}H NMR spectra. Indeed, the detection of a very broad peak centered at around 1.47 ppm in the *in situ* ^{1}H NMR spectrum (Figure 8b), recorded on 24 h hydrated sample, is in very good agreement with the formation of ettringite. The very broad nature of the resonance for hydroxyls in ettringite is probably due to their diverse local environments leading to substantial chemical shift distributions. Moreover, at early hydration stages, fast deuterium-proton exchange between O−H and D_2O groups can weaken the peak intensity coupled to the hydroxyls in the *in situ* NMR spectra. In addition, the broad peaks in the range 1 to 5 ppm are also clearly evident, especially at later hydration

https://doi.org/10.1021/acs.jpcc.1c00984
J. Phys. Chem. C 2021, 125, 9261−9272

stages, which are due to the hydrated aluminate phases such as aluminum hydroxide gel and ettringite.

Aluminum hydroxide gel has been detected throughout the course of the *in situ* study with its characteristic peaks at 4.2 and 5.9 ppm as well as in the 2−4 ppm range. In addition, the broad peak in the range 4 to 7 ppm also contributes to the amorphous aluminum hydroxide gel structure. The relatively broad, poorly resolved, and featureless ^{1}H NMR spectra that span a chemical shift range of ca. 1−7 ppm for aluminum hydroxide gel reflect the high heterogeneous distribution of the immediate local molecular environments. This study elucidates the mutual hydrogen-bonding networks formed by intralayer hydroxyls, while unraveling the absence of interlayer hydrogen bonding of hydroxyls in general. The emerging structural description of the aluminum hydroxide gel is that the chemical identity and the 2D layered framework arrangement is similar to gibbsite; however, the further stacking of layers in the third dimension, responsible for the long-range order, is absent. The interlayer galleries are water-rich, probably due to their noncovalent interactions with the external hydroxyls; that governs the short-range order and the predominant drive in stabilizing the amorphous aluminum hydroxide gel. Calcium ions may also reside in this gallery by interacting with the hydroxyls or water molecules and influence the local ^{27}Al molecular environments as has been echoed on the quadrupolar coupling parameters and isotropic chemical shifts as shown in Table 1.

A close examination of the *in situ* ^{1}H MAS NMR spectra of hydrated samples, especially in neat ye'elimite that have completed at least 20 h of hydration process, highlighted the absence of intense water resonance peak. Hence, it is clear that there has been no more water present in the pastes that could have hydrated the remaining anhydrous ye'elimite. It is important to note here that, for this study, the amount of water (or rather the w/s ratio, 0.5) was chosen in such a manner that it has been well below the required stoichiometric amounts. The theoretical w/s ratio, when deuterated water is employed, for the complete hydration of ye'elimite would be 0.59 and 1.11 according to eq 1 and 2, respectively. On the other hand, by increasing the water to ye'elimite ratio with the employment of a nonreactive filler (calcium carbonate) in the mix resulted in a faster initial reaction rate and higher product formation (Figure S4), validating the *in situ* NMR experimental approach employed in this study. Although a variety of transient species have been detected during the *in situ* investigations, only lower amounts have been accounted at any given time as their oversaturation resulted in the precipitation of stable hydrated phases.

CONCLUSIONS

This study has successfully illustrated the two reaction pathways adopted by orthorhombic ye'elimite upon very early hydration, one in which monosulfate and aluminum hydroxide precipitated in the absence of calcium sulfate and the other pathway in which ettringite and aluminum hydroxide resulted in the presence of calcium sulfate. The traces of ettringite detected during the very early hydration, in the absence of calcium sulfate, is due to the reactions of minor quantity of monocalcium aluminate present in the sample. The direct observation of transient species such as naked hydroxides, tetracalcium aluminate anions, and hydrated calcium aluminates such as hydrogarnet (katoite) during the mapping of very early hydration stages of calcium aluminates and calcium sulfoaluminates revealed the potentials of a newly designed time-resolved *in situ* multinuclear MAS NMR experimental approach.

The *in situ* ^{1}H NMR snapshots recorded every few seconds have been sufficient to unravel, in a unprecedented detail, the intense chemical and microstructural activities, competitions in dissolution processes, phase transition of metastable phases, and product formations during the early hydration stages of ye'elimite. The multicomponent, heterogeneous, and non-equilibrium system resulted from the hydration of ye'elimite, in the presence of calcium sulfate, has been successfully fingerprinted by *in situ* ^{1}H MAS NMR spectroscopy, and the approach can be expanded to many complex material science fields. In addition, we have demonstrated that the complementary and fast *in situ* ^{27}Al MAS NMR has the unparalleled ability to equally detect and quantify amorphous, crystalline, and disordered phases as well as surface species formed during the hydration process. The combined time-resolved *in situ* ^{1}H and ^{27}Al MAS NMR experimental approach implemented in this study has been successful in monitoring the hydration of monocalcium aluminate and ye'elimite, nucleation and precipitation of transient species, and finally, their transformation and crystallization into stable hydrated aluminate and sulfoaluminate phases, concurrently.

ASSOCIATED CONTENT

Supporting Information

The Supporting Information is available free of charge at https://pubs.acs.org/doi/10.1021/acs.jpcc.1c00984.

Powder X-ray diffraction pattern, ^{27}Al MAS and MQMAS NMR data, thermogravimetric/differential scanning calorimetric patterns, and SEM micrograph of anhydrous orthorhombic ye'elimite (PDF)

AUTHOR INFORMATION

Corresponding Author

Leonardo Marchese − *Dipartimento di Scienze ed Innovazione Tecnologica, Università del Piemonte Orientale, 15121 Alessandria, Italy;* orcid.org/0000-0001-9191-1237; Email: leonardo.marchese@uniupo.it

Authors

Geo Paul − *Dipartimento di Scienze ed Innovazione Tecnologica, Università del Piemonte Orientale, 15121 Alessandria, Italy;* orcid.org/0000-0002-0944-0016

Enrico Boccaleri − *Dipartimento di Scienze ed Innovazione Tecnologica, Università del Piemonte Orientale, 15121 Alessandria, Italy*

Claudio Cassino − *Dipartimento di Scienze ed Innovazione Tecnologica, Università del Piemonte Orientale, 15121 Alessandria, Italy;* orcid.org/0000-0002-7785-2717

Daniela Gastaldi − *Buzzi Unicem S.p.A., 15033 Casale Monferrato, AL, Italy*

Luigi Buzzi − *Buzzi Unicem S.p.A., 15033 Casale Monferrato, AL, Italy*

Fulvio Canonico − *Buzzi Unicem S.p.A., 15033 Casale Monferrato, AL, Italy*

Complete contact information is available at: https://pubs.acs.org/10.1021/acs.jpcc.1c00984

Author Contributions

The manuscript was written through contributions of all authors. All authors have given approval to the final version of the manuscript.

Notes

The authors declare no competing financial interest.

■ ACKNOWLEDGMENTS

The authors would like to thank the anonymous reviewers for their valuable comments which helped to improve the manuscript. We thank Valentino Merlo and Federico Begni for useful discussions.

■ REFERENCES

(1) Pedersen, M. T.; Jensen, F.; Skibsted, J. Structural Investigation of Ye'elimite, $Ca_4Al_6O_{12}SO_4$, by ^{27}Al MAS and MQMAS NMR at Different Magnetic Fields. *J. Phys. Chem. C* **2018**, *122*, 12077−12089.

(2) Scrivener, K. L.; John, V. M.; Gartner, E. M.; UN Environment. Eco-efficient Cements: Potential Economically Viable Solutions for a Low-CO_2 Cement-Based Materials Industry. *Cem. Concr. Res.* **2018**, *114*, 2−26.

(3) Monteiro, P. J. M.; Miller, S. A.; Horvath, A. Towards Sustainable Concrete. *Nat. Mater.* **2017**, *16*, 698−699.

(4) Sharp, J. H.; Lawrence, C. D.; Yang, R. Calcium Sulfoaluminate Cements - Low Energy Cements, Special Cements or What? *Adv. Cem. Res.* **1999**, *11*, 3−13.

(5) Gastaldi, D.; Canonico, F.; Capelli, L.; Bianchi, M.; Pace, M. L.; Telesca, A.; Valenti, G. L. Hydraulic Behaviour of Calcium Sulfoaluminate Cement Alone and in Mixture with Portland Cement. In *XIII International Congress on the Chemistry of Cement*; Madrid, 2011; p 381.

(6) Klein, A. Calciumaluminosulfate and Expansive Cements Containing same. U.S. Patent US 3,155,526, 1963.

(7) Hargis, C. W.; Moon, J.; Lothenbach, B.; Winnefeld, F.; Wenk, H.-R.; Monteiro, P. J. M. Calcium Sulfoaluminate Sodalite ($Ca_4Al_6O_{12}SO_4$) Crystal Structure Evaluation and Bulk Modulus Determination. *J. Am. Ceram. Soc.* **2014**, *97*, 892−898.

(8) Paul, G.; Boccaleri, E.; Marchese, L.; Buzzi, L.; Canonico, F.; Gastaldi, D. Low Temperature Sulfoaluminate Clinkers: The Role of Sulfates and Silicates on the Different Hydration Behavior. *Constr. Build. Mater.* **2021**, *268*, 121111.

(9) Beretka, J.; de Vito, B.; Santoro, L.; Sherman, N.; Valenti, G. L. Utilization of Industrial Wastes and By-Products for the Synthesis of Special Cements. *Resour. Conserv. Recy.* **1993**, *9*, 179.

(10) Buzzi, L.; Canonico, F.; Schäffel, P. Investigation on High-Performance Concrete Based on Calcium Sulfoaluminate Cement. In *XIII International Congress on the Chemistry of Cement*; Madrid, 2011; p 152.

(11) Calos, N. J.; Kennard, C. H. L.; Whittaker, A. K.; Davis, R. L. Structure of Calcium Aluminate Sulfate $Ca_4Al_6O_{16}S$. *J. Solid State Chem.* **1995**, *119*, 1−7.

(12) Cuesta, A.; De la Torre, A. G.; Losilla, E. R.; Peterson, V. K.; Rejmak, P.; Ayuela, A.; Frontera, C.; Aranda, M. A. G. Structure, Atomistic Simulations, and Phase Transition of Stoichiometric Yeelimite. *Chem. Mater.* **2013**, *25*, 1680−1687.

(13) Bullerjahn, F.; Zajac, M.; Ben Haha, M. Effect of Raw Mix Design and of Clinkering Process on the Formation and Mineralogical Composition of (Ternesite) Belite Calcium Sulphoaluminate Ferrite Clinker. *Mater. Struct.* **2015**, *48*, 3895−3911.

(14) Cuesta, A.; Álvarez-Pinazo, G.; Sanfélix, S. G.; Peral, I.; Aranda, M. A. G.; De la Torre, A. G. Hydration Mechanisms of Two Polymorphs of Synthetic Ye'elimite. *Cem. Concr. Res.* **2014**, *63*, 127−136.

(15) Martin, L. H. J.; Winnefeld, F.; Müller, C. J.; Lothenbach, B. Contribution of Limestone to the Hydration of Calcium Sulfoaluminate Cement. *Cem. Concr. Compos.* **2015**, *62*, 204−211.

(16) Winnefeld, F.; Lothenbach, B. Hydration of Calcium Sulfoaluminate Cements - Experimental Findings and Thermodynamic Modelling. *Cem. Concr. Res.* **2010**, *40*, 1239−1247.

(17) Winnefeld, F.; Lothenbach, B. Phase Equilibria in the System $Ca_4Al_6O_{12}SO_4$ - Ca_2SiO_4 - $CaSO_4$ - H_2O Referring to the Hydration of Calcium Sulfoaluminate Cements. *RILEM Technol. Lett.* **2016**, *1*, 10−16.

(18) Bullerjahn, F.; Boehm-Courjault, E.; Zajac, M.; Ben Haha, M.; Scrivener, K. L. Hydration Reactions and Stages of Clinker Composed Mainly of Stoichiometric Ye'elimite. *Cem. Concr. Res.* **2019**, *116*, 120−133.

(19) Glasser, F. P.; Zhang, L. High-Performance Cement Matrices Based on Calcium Sulfoaluminate-Belite Compositions. *Cem. Concr. Res.* **2001**, *31*, 1881−1886.

(20) Rawal, A.; Smith, B. J.; Athens, G. L.; Edwards, C. L.; Roberts, L.; Gupta, V.; Chmelka, B. F. Molecular Silicate and Aluminate Species in Anhydrous and Hydrated Cements. *J. Am. Chem. Soc.* **2010**, *132*, 7321−7337.

(21) Hughes, C. E.; Harris, K. D. M. A Technique for In Situ Monitoring of Crystallization from Solution by Solid-State ^{13}C CPMAS NMR Spectroscopy. *J. Phys. Chem. A* **2008**, *112*, 6808−6810.

(22) Hughes, C. E.; Harris, K. D. M. Direct Observation of a Transient Polymorph During Crystallization. *Chem. Commun.* **2010**, *46*, 4982−4984.

(23) Cerreia Vioglio, P.; Mollica, G.; Juramy, M.; Hughes, C. E.; Williams, P. A.; Ziarelli, F.; Viel, S.; Thureau, P.; Harris, K. D. M. Insights into the Crystallization and Structural Evolution of Glycine Dihydrate by In Situ Solid-State NMR Spectroscopy. *Angew. Chem., Int. Ed.* **2018**, *57*, 6619−6623.

(24) Hughes, C. E.; Williams, P. A.; Harris, K. D. M. CLASSIC NMR": An In-Situ NMR Strategy for Mapping the Time-Evolution of Crystallization Processes by Combined Liquid-State and Solid-State Measurements. *Angew. Chem., Int. Ed.* **2014**, *53*, 8939−8943.

(25) Hughes, C. E.; Walkley, B.; Gardner, L. J.; Walling, S. A.; Bernal, S. A.; Iuga, D.; Provis, J. L.; Harris, K. D. M. Exploiting In-Situ Solid-State NMR Spectroscopy to Probe the Early Stages of Hydration of Calcium Aluminate Cement. *Solid State Nucl. Magn. Reson.* **2019**, *99*, 1−6.

(26) Pustovgar, E.; Sangodkar, R. P.; Andreev, A. S.; Palacios, M.; Chmelka, B. F.; Flatt, R. J.; d'Espinose de Lacaillerie, J.-B. Understanding Silicate Hydration from Quantitative Analyses of Hydrating Tricalcium Silicates. *Nat. Commun.* **2016**, *7*, 10952.

(27) Pustovgar, E.; Mishra, R. K.; Palacios, M.; d'Espinose de Lacaillerie, J.-B.; Matschei, T.; Andreev, A. S.; Heinz, H.; Verel, R.; Flatt, R. J. Influence of Aluminates on the Hydration Kinetics of Tricalcium Silicate. *Cem. Concr. Res.* **2017**, *100*, 245−262.

(28) Irico, S.; Bovio, A. G.; Paul, G.; Boccaleri, E.; Gastaldi, D.; Marchese, L.; Buzzi, L.; Canonico, F. A solid-State NMR and X-ray Powder Diffraction Investigation of the Binding Mechanism for Self-Healing Cementitious Materials Design: the Assessment of the Reactivity of Sodium Silicate Based Systems. *Cem. Concr. Compos.* **2017**, *76*, 57−63.

(29) Edén, M. ^{27}Al NMR Studies of Aluminosilicate Glasses. *Annu. Rep. NMR Spectrosc.* **2015**, *86*, 237−331.

(30) Frydman, L.; Harwood, J. S. Isotropic Spectra of Half-Integer Quadrupolar Spins from Bidimensional Magic-Angle Spinning NMR. *J. Am. Chem. Soc.* **1995**, *117*, 5367−5368.

(31) Amoureux, J. P.; Fernandez, C.; Steuernagel, S. Z Filtering in MQMAS NMR. *J. Magn. Reson., Ser. A* **1996**, *123*, 116−118.

(32) Yesinowski, J. P.; Eckert, H.; Rossman, G. R. Characterization of Hydrous Species in Minerals by High-speed ^1H MAS-NMR. *J. Am. Chem. Soc.* **1988**, *110*, 1367−1375.

(33) Brown, S. P. Applications of High-Resolution ^1H Solid-State NMR. *Solid State Nucl. Magn. Reson.* **2012**, *41*, 1−27.

(34) MacKenzie, K. J. D.; Smith, M. E. *Multinuclear Solid-State NMR of Inorganic Materials*, 1st ed.; Pergamon Materials Series 6; Pergamon: London, 2002.

https://doi.org/10.1021/acs.jpcc.1c00984
J. Phys. Chem. C 2021, 125, 9261−9272

(35) Winnefeld, F.; Barlag, S. Calorimetric and Thermogravimetric Study on the Influence of Calcium Sulfate on the Hydration of Ye'elimite. *J. Therm. Anal. Calorim.* **2010**, *101*, 949−957.
(36) Massiot, D.; Fayon, F.; Capron, M.; King, I.; Le Calve, S.; Alonso, B.; Durand, J.-O.; Bujoli, B.; Gan, Z.; Hoatson, G. Modelling One- and Two-Dimensional Solid-State NMR Spectra. *Magn. Reson. Chem.* **2002**, *40*, 70−75.
(37) Paul, G.; Boccaleri, E.; Buzzi, L.; Canonico, F.; Gastaldi, D. Friedel's Salt Formation in Sulfoaluminate Cements: A Combined XRD and ^{27}Al MAS NMR Study. *Cem. Concr. Res.* **2015**, *67*, 93−102.
(38) Skibsted, J.; Henderson, E.; Jakobsen, H. Characterization of Calcium Aluminate Phases in Cements by ^{27}Al MAS NMR Spectroscopy. *Inorg. Chem.* **1993**, *32*, 1013−1027.
(39) Skibsted, J.; Pedersen, M. T.; Holzinger, J. Resolution of the Two Aluminum Sites in Ettringite by ^{27}Al MAS and MQMAS NMR at Very High Magnetic Field (22.3 T). *J. Phys. Chem. C* **2017**, *121*, 4011−4017.
(40) Pena, P.; Rivas Mercury, J. M.; de Aza, A. H.; Turrillas, X.; Sobrados, I.; Sanz, J. Solid-state ^{27}Al and ^{29}Si NMR Characterization of Hydrates Formed in Calciumaluminate-Silica Fume Mixtures. *J. Solid State Chem.* **2008**, *181*, 1744−1752.
(41) Faucon, P.; Charpentier, T.; Bertrandie, D.; Nonat, A.; Virlet, J.; Petit, J. C. Characterization of Calcium Aluminate Hydrates and Related Hydrates of Cement Pastes by ^{27}Al MQ-MAS NMR. *Inorg. Chem.* **1998**, *37*, 3726−3733.
(42) Walkley, B.; Provis, J. L. Solid-State Nuclear Magnetic Resonance Spectroscopy of Cements. *Mater. Today Adv.* **2019**, *1*, 100007.
(43) Gastaldi, D.; Paul, G.; Marchese, L.; Irico, S.; Boccaleri, E.; Mutke, S.; Buzzi, L.; Canonico, F. Hydration Products in Sulfoaluminate Cements: Evaluation of Amorphous Phases by XRD/Solid-State NMR. *Cem. Concr. Res.* **2016**, *90*, 162−173.
(44) Gastaldi, D.; Bertola, F.; Canonico, F.; Buzzi, L.; Mutke, S.; Irico, S.; Paul, G.; Marchese, L.; Boccaleri, E. A Chemical/Mineralogical Investigation of the Behavior of Sulfoaluminate Binders Submitted to Accelerated Carbonation. *Cem. Concr. Res.* **2018**, *109*, 30−41.
(45) Gastaldi, D.; Bertola, F.; Irico, S.; Paul, G.; Canonico, F. Hydration Behavior of Cements with Reduced Clinker Factor in Mixture with Sulfoaluminate Binder. *Cem. Concr. Res.* **2021**, *139*, 106261.
(46) Zajac, M.; Skocek, J.; Bullerjahn, F.; Lothenbach, B.; Scrivener, K.; Ben Haha, M. Early Hydration of Ye'elimite: Insights from Thermodynamic Modelling. *Cem. Concr. Res.* **2019**, *120*, 152−163.
(47) Jansen, D.; Spies, A.; Neubauer, J.; Ectors, D.; Goetz-Neunhoeffer, F. Studies on the Early Hydration of Two Modifications of Ye'elimite with Gypsum. *Cem. Concr. Res.* **2017**, *91*, 106−116.
(48) Jansen, D.; Wolf, J. J.; Fobbe, N. The Hydration of Nearly Pure Ye'elimite with a Sulfate Carrier in a Stoichiometric Ettringite Binder System. Implications for the Hydration Process Based on In-Situ XRD, ^{1}H-TD-NMR, Pore Solution Analysis, and Thermodynamic Modelling. *Cem. Concr. Res.* **2020**, *127*, 105923.
(49) Zhang, Y.; Chang, J.; Zhao, J.; Fang, Y. Nanostructural Characterization of $Al(OH)_3$ Formed During the Hydration of Calcium Sulfoaluminate Cement. *J. Am. Ceram. Soc.* **2018**, *101*, 4262−4274.
(50) Chang, J.; Zhang, Y.; Shang, X.; Zhao, J.; Yu, X. Effects of Amorphous AH_3 Phase on Mechanical Properties and Hydration Process of $C_4A_3$$-CH_2-CH-H_2O System. *Constr. Build. Mater.* **2017**, *133*, 314−322.
(51) Baquerizo, L. G.; Matschei, T.; Scrivener, K. L.; Saeidpour, M.; Wadsö, L. Hydration States of AFm Cement Phases. *Cem. Concr. Res.* **2015**, *73*, 143−157.
(52) Taylor, H. F. W. *Cement Chemistry*, 2nd ed.; Thomas Telford: London, 1997.
(53) Bertola, F.; Gastaldi, D.; Canonico, F.; Paul, G. CSA and Slag: Towards CSA Composite Binders. *Adv. Cem. Res.* **2019**, *31*, 147−158.
(54) Cuesta, A.; De la Torre, A. G.; Santacruz, I.; Trtik, P.; Da Silva, J. C.; Diaz, A.; Holler, M.; Aranda, M. A. G. Chemistry and Mass Density of Aluminum Hydroxide Gel in Eco-Cements by Ptychographic X-ray Computed Tomography. *J. Phys. Chem. C* **2017**, *121*, 3044−3054.
(55) Song, F.; Yu, Z.; Yang, F.; Lu, Y.; Liu, Y. Microstructure of Amorphous Aluminum Hydroxide in Belite-Calcium Sulfoaluminate Cement. *Cem. Concr. Res.* **2015**, *71*, 1−6.
(56) Zhang, Y.; Chang, J.; Zhao, J. Microstructural Comparison of the AH_3 Phase in the Hydration of Three Structural Modifications of Ye'elimite. *J. Am. Ceram. Soc.* **2018**, *102*, 2165−2175.
(57) Sandström, D. E.; Jarlbring, M.; Antzutkin, O. N.; Forsling, W. A Spectroscopic Study of Calcium Surface Sites and Adsorbed Iron Species at Aqueous Fluorapatite by Means of ^{1}H and ^{31}P MAS NMR. *Langmuir* **2006**, *22*, 11060−11064.
(58) Méducin, F.; Bresson, B.; Lequeux, N.; de Noirfontaine, M.-N.; Zanni, H. Calcium Silicate Hydrates Investigated by Solid-State High Resolution ^{1}H and ^{29}Si Nuclear Magnetic Resonance. *Cem. Concr. Res.* **2007**, *37*, 631−638.
(59) Engelhardt, G.; Sieger, P.; Felsche, J. Dynamic Proton Exchange in the Hydrogen Dihydroxide Ion $H_3O_2^-$ of the Hydroxosodalite Hydrate $[Na_4(H_3O_2)]_2[SiAlO_4]_6$: ^{1}H MAS NMR Spectroscopic Evidence. *Angew. Chem., Int. Ed. Engl.* **1992**, *31*, 1210−1212.
(60) Engelhardt, G.; Felsche, J.; Sieger, P. The Hydrosodalite System $Na_{6+x}[SiAlO_4]_6(OH)_x\cdot nH_2O$: Formation, Phase Composition, and De- and Rehydration Studied by ^{1}H, ^{23}Na, and ^{29}Si MAS-NMR Spectroscopy in Tandem with Thermal Analysis, X-ray Diffraction, and IR Spectroscopy. *J. Am. Chem. Soc.* **1992**, *114*, 1173−1182.
(61) Wiebcke, M.; Engelhardt, G.; Felsche, J.; Kempa, P. B.; Sieger, P.; Schefer, J.; Fischer, P. Orientational Disorder of the Hydrogen Dihydroxide Anion, $O_2H_3^-$, in Sodium Hydroxosodalite Dihydrate, $Na_8[Al_8Si_8O_{24}](OH)_2\cdot 2H_2O$: Single-Crystal X-ray and Powder Neutron Diffraction and MAS NMR and FT IR Spectroscopy. *J. Phys. Chem.* **1992**, *96*, 392−397.
(62) Hansen, M. R.; Jakobsen, H. J.; Skibsted, J. Structure and Dynamics of Hydrous Surface Species on Alumina-Boria Catalysts and Their Precursors from ^{1}H, ^{2}H, ^{11}B, and ^{27}Al MAS NMR Spectroscopy. *J. Phys. Chem. C* **2009**, *113*, 2475−2486.
(63) Paul, G.; Bisio, C.; Braschi, I.; Cossi, M.; Gatti, G.; Gianotti, E.; Marchese, L. Combined Solid-State NMR, FT-IR and Computational Studies on Layered and Porous Materials. *Chem. Soc. Rev.* **2018**, *47*, 5684−5739.
(64) Okoronkwo, M. U.; Glasser, F. P. Compatibility of Hydrogarnet, $Ca_3Al_2(SiO_4)_x(OH)_{4(3-x)}$, with Sulfate and Carbonate-Bearing Cement Phases: 5−85 °C. *Cem. Concr. Res.* **2016**, *83*, 86−96.
(65) Fitzgerald, J. J.; Piedra, G.; Dec, S. F.; Seger, M.; Maciel, G. E. Dehydration Studies of a High-Surface-Area Alumina (Pseudoboehmite) Using Solid-State ^{1}H and ^{27}Al NMR. *J. Am. Chem. Soc.* **1997**, *119*, 7832−7842.
(66) Vyalikh, A.; Zesewitz, K.; Scheler, U. Hydrogen Bonds and Local Symmetry in the Crystal Structure of Gibbsite. *Magn. Reson. Chem.* **2010**, *48*, 877−881.

https://doi.org/10.1021/acs.jpcc.1c00984
J. Phys. Chem. C 2021, 125, 9261−9272